Available online at www.sciencedirect.com
ScienceDirect
Catalysis Today 136 (2008) 235–242
CATALYSIS TODAY
www.elsevier.com/locate/cattod

# Study of the performance of $Mo_2C$ for *iso*-octane steam reforming

Oscar G. Marin Flores, Su Ha *

*Washington State University, Department of Chemical Engineering, P.O. Box 642710, Pullman, WA 99164-2710, USA*

Available online 25 March 2008

**Abstract**

In the present work, the performance of commercial molybdenum carbide ($Mo_2C$) for isooctane steam reforming has been investigated in order to determine the effects of major operating parameters (temperature, space velocity, and steam to carbon ratio) on the catalytic activity. While the results obtained indicate an onset reforming temperature of 850 °C, high concentrations of $H_2$ in the reforming environment were found to reduce the onset temperature to 750 °C. The catalytic activity at 850 °C was sufficient to produce hydrogen yields greater than 90% and carbon conversions close to 100%, with a low selectivity to $CH_4$ and $CO_2$. In addition, and consistent with thermodynamic predictions, a steam to carbon ratio of 1 appeared to optimize the reforming rates. Finally, based on experimental observations, a reaction mechanism was formulated and used to interpret the results obtained during catalytic activity measurements. This mechanism involves continuous oxidation and reduction of Mo metal, which can provide activity and stability to the catalyst when occurring at similar rates.


*Keywords:* Molybdenum carbide; Isooctane steam reforming; Activity; XRD; XPS

## 1. Introduction

Polymer electrolyte membrane (PEM) fuel cells have emerged as a promising energy alternative for satisfying the growing demands of the transportation industry. No other energy conversion technology offers the combination of benefits that fuel cells do. Specifically, high energy efficiency and reduced greenhouse gas emissions are some of the features that make this technology a highly attractive power source for future generation vehicles [1].

Hydrogen is considered the ideal fuel for PEM fuel cells because it produces simple power-generating systems with high energy efficiency and a fast response time [2,3]. To achieve this high performance PEM fuel cells require high purity hydrogen and, consequently, efforts have been primarily focused on the development of a readily available source of pure hydrogen. Two different pathways are currently under development to address this issue. The first one consists of off-board production of pure hydrogen, followed by a convenient storage method which allows this stored hydrogen to be used by the fuel cell when needed. Alternatively, the second one entails on-demand generation of hydrogen, which occurs via an on-board fuel processor capable of transforming a variety of feedstocks into high-purity hydrogen.

At present, technologies employed for the storage of hydrogen produced off-board continue to be cost-prohibitive and also present further drawbacks. For instance, storage of practical amounts of compressed hydrogen gas requires very large high-pressure vessels; liquid hydrogen storage suffers significant evaporative loss; metal hydride systems have low hydrogen storage density; and carbon nanotubes do not yet have practical applications because of high cost and low hydrogen storage density [4]. In addition, no hydrogen fuel supply infrastructure currently exists and much development is needed before a practical infrastructure can be created [4,5]. Conversely, high-energy-density fossil fuels already have an existing low-cost infrastructure for fuel storage and delivery. Thus, the on-board production of hydrogen using fossil fuels represents an interesting alternative to fulfill the requirements of hydrogen for fuel cell applications.

On-board hydrogen production is typically performed in a fuel processor, which consists of a reformer unit followed by several reactors designed to minimize sulfur and CO contents of the product stream. Methanol, gasoline, and diesel are some of the liquid fuels considered to be attractive options as potential hydrogen sources. However, gasoline appears to make the most

* Corresponding author. Tel.: +1 509 335 3786.
*E-mail address:* suha@wsu.edu (S. Ha).

0920-5861/$ – see front matter 
doi:10.1016/j.cattod.2008.02.004

economic and practical sense. Well-known advantages of gasoline are its plentiful supply, its relatively low price, the ease and safety of handling it, and its high energy density. Moreover, a highly efficient production and distribution infrastructure is already in operation globally.

Steam reforming, autothermal reforming, and partial oxidation are the primary methods used in hydrocarbon processing for hydrogen production in fuel cell applications. Of these reforming options, endothermic steam reforming is the most common technique, as it produces higher hydrogen concentrations in the crude reformate gas compared to partial oxidation and autothermal reforming [6–8]. Steam reforming of liquid hydrocarbons is largely carried out over Ni-based catalysts, and results describing their performance have been reported elsewhere [9,10]. It has been found that these catalysts exhibit good activity and selectivity at high temperatures, but that their stability appears to diminish due to sintering. Addition of palladium to Ni-catalyst composition has been determined to cause a significant improvement in the performance. Steam reforming catalysts based on costly precious metals (platinum, ruthenium, rhodium, rhenium) have been reported to be more effective for hydrocarbon steam reforming as they preclude carbon deposition and inhibit methane formation [11]. Nonetheless, the high expenses required even for small loadings of noble metal prevent these catalysts from extensive usage. More recently, early transition metal carbides have attracted much attention for displaying catalytic properties similar to those of noble metals [12]. Previous studies indicate that bulk molybdenum carbide ($Mo_2C$) catalysts show high coke resistance at low steam to carbon ratios as well as good sulfur tolerance for both methane and isooctane steam reforming [14,15]. These properties together with high thermal stability and low cost make $Mo_2C$ an interesting alternative catalyst for gasoline steam reforming.

The present investigation is intended to study the performance of $Mo_2C$ as a catalyst for gasoline steam reforming under different operating conditions. Since gasoline is a complex mixture of hydrocarbons, the analysis was simplified by using isooctane as gasoline surrogate. The experimental results reported in this work will be analyzed in order to determine the effect of the operating parameters on the catalytic activity. In turn, the resulting analysis will allow us to formulate a reaction mechanism, which facilitates better understanding of the catalytic behavior of $Mo_2C$ when used for isooctane steam reforming.

## 2. Thermodynamic analysis

Hydrogen production via steam reforming of isooctane ($C_8H_{18}$) is an endothermic process, which can be expressed as follows:

$$C_8H_{18} + 8H_2O \rightarrow 8CO + 17H_2 \quad \Delta H^\circ = 1274.9\,\text{kJ mol}^{-1} \tag{1}$$

It is generally accepted that steam reforming is the net result of a series of elementary reactions, for some of which the catalyst surface plays a significant role. The equilibrium composition of the reformate can be estimated by minimizing the Gibbs free energy. This method does not demand knowledge of the exact chemical kinetics leading to the equilibrium; instead, it only requires the identity of the chemical compounds existing in the equilibrium state.

The equilibrium compositions of Fig. 1 show the effect of the temperature on the reformer performance. High temperatures increase the efficiency of the reformer, as indicated by the rise in the hydrogen yield, which in turn is due to the decline in the concentrations of methane and unreacted water. As the temperature increases, the equilibrium compositions approximate the values dictated by the stoichiometry of reaction (1), i.e., 32% for CO and 68% for $H_2$, which indicates that reaction (1) is approaching completion.

Fig. 2 displays the effect of the steam to carbon molar ratio (S/C) on the hydrogen yield, which suggests that the production of hydrogen can be optimized by using S/C ratios near 1. This result is in agreement with the stoichiometry of reaction (1) and seems to indicate that excess steam is not favorable for the process since it will increase the amount of unreacted water.

## 3. Experimental

Experiments were performed in a 12 mm fixed-bed tubular (quartz) reactor. A schematic of the system used is shown in Fig. 3. The liquid feed, consisting of water and isooctane, was vaporized at 200 °C and mixed along with the carrier gas in a vaporizer containing a silicon carbide bed to enhance the mixing. Calibrated syringe pumps and mass flow controllers were employed to control the flow rates. The operating temperature range of the reactor was 650 °C −1000 °C, and the high-temperature exit stream was cooled down to 5 °C to separate water, non-reacted isooctane, and other possible condensable compounds from the off-gas. The dry gas product was analyzed using an SRI chromatograph to monitor $H_2$, CO, $CO_2$, and $CH_4$ concentrations.

The catalysts employed were $Mo_2C$ (Stock # 12192, Lot # L09Q054) and $MoO_2$ (Stock # 48117, Lot # B11P16), which were purchased from Alfa Aesar. Typically, 0.5 g of catalyst

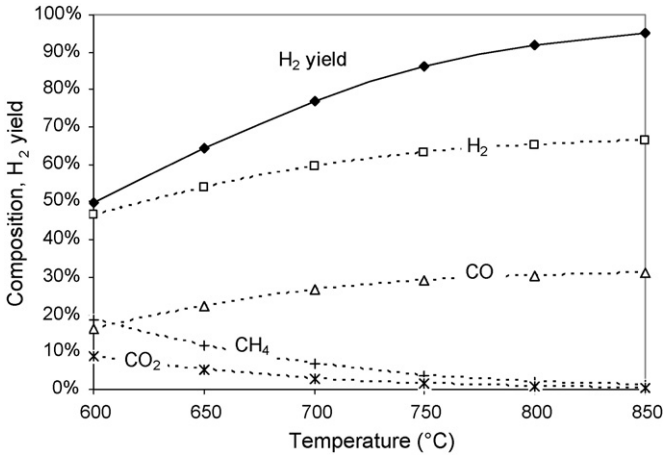


Fig. 1. Equilibrium compositions as a function of temperature.

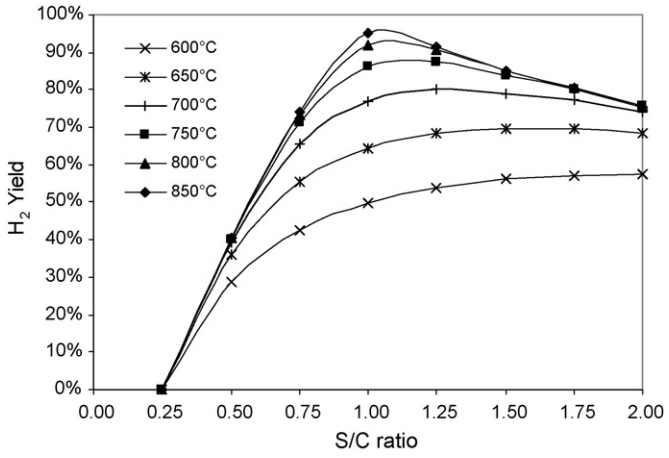


Fig. 2. Hydrogen yield as a function of temperature and S/C ratio.

was used in each reforming experiment. The catalyst sample was supported by a quartz wool plug placed inside the reactor as shown in Fig. 3. The spent samples were analyzed by powder X-ray diffraction (XRD) on two different instruments: a Philips diffractometer using Co Kα radiation with an iron filter, and a Siemens D-500 X-ray powder diffractometer with Cu Kα radiation. XPS spectra were obtained with an AXIS-165 manufactured by Kratos Analytical Inc., using an achromatic Mg Kα (1254 eV) X-ray radiation with a power of 210 W. The binding energy was calibrated against the $4f_{7/2}$ line of clean Au to be at 84 eV. A pass energy (PE) of 80 eV was used to acquire all survey scans. At this PE the energy resolution was about 1.2 eV. The high resolution spectra of Mo 3d were acquired at PE of 40 eV with an energy resolution of about 0.8 eV. The base pressure of the XPS analyzing chamber was $1.0 \times 10^{-9}$ torr. As a preliminary preparation for XPS analysis, the powdered samples were pressed into pure Indium (99.99 pure) and analyzed in order to minimize the effects of charging. The curve fitting of high-resolution spectra was performed using a least-squares fitting program permitting linear or Shirley fitted backgrounds, a mixture of Gaussian and Lorentzian peak shapes, constraints on spin-orbit splitting intervals and spin-orbit pair area ratios, as well as constraints on peak position (binding energy), and peak width. Mo3d spin-orbit pair intervals were set at 3.13 eV, and an area ratio of 0.666 was used. To prevent further oxidation between the end of the experiment and the XPS or XRD analysis, the samples were cooled down to room temperature inside the reactor using helium gas flow.

BET surface area measurements were performed using a Coulter SA-3100 automated characterization machine.

The data was analyzed in terms of hydrogen yield, carbon conversion, water conversion and selectivities, which were calculated as follows:

$$\mathrm{H_2\ yield} = \frac{2 \times n^{\mathrm{out}}_{\mathrm{H_2}}}{2 \times n^{\mathrm{in}}_{\mathrm{H_2O}} + 18 \times n^{\mathrm{in}}_{\mathrm{C_8H_{18}}}}$$

$$\mathrm{C\ conversion} = \frac{n^{\mathrm{out}}_{\mathrm{CH_4}} + n^{\mathrm{out}}_{\mathrm{CO}} + n^{\mathrm{out}}_{\mathrm{CO_2}}}{8 \times n^{\mathrm{in}}_{\mathrm{C_8H_{18}}}}$$

$$\mathrm{H_2O\ conversion} = \frac{n^{\mathrm{out}}_{\mathrm{CO}} + 2n^{\mathrm{out}}_{\mathrm{CO_2}}}{n^{\mathrm{in}}_{\mathrm{H_2O}}}$$

$$\mathrm{H_2\ selectivity} = \frac{n^{\mathrm{out}}_{\mathrm{H_2}}}{n^{\mathrm{out}}_{\mathrm{H_2}} + n^{\mathrm{out}}_{\mathrm{CO}} + n^{\mathrm{out}}_{\mathrm{CO2}} + n^{\mathrm{out}}_{\mathrm{CH_4}}}$$

$$\mathrm{CO\ selectivity} = \frac{n^{\mathrm{out}}_{\mathrm{CO}}}{n^{\mathrm{out}}_{\mathrm{H_2}} + n^{\mathrm{out}}_{\mathrm{CO}} + n^{\mathrm{out}}_{\mathrm{CO_2}} + n^{\mathrm{out}}_{\mathrm{CH_4}}}$$

$$\mathrm{CO_2\ selectivity} = \frac{n^{\mathrm{out}}_{\mathrm{CO_2}}}{n^{\mathrm{out}}_{\mathrm{H_2}} + n^{\mathrm{out}}_{\mathrm{CO}} + n^{\mathrm{out}}_{\mathrm{CO_2}} + n^{\mathrm{out}}_{\mathrm{CH_4}}}$$

$$\mathrm{CH_4\ selectivity} = \frac{n^{\mathrm{out}}_{\mathrm{CH_4}}}{n^{\mathrm{out}}_{\mathrm{H2}} + n^{\mathrm{out}}_{\mathrm{CO}} + n^{\mathrm{out}}_{\mathrm{CO_2}} + n^{\mathrm{out}}_{\mathrm{CH_4}}}$$

## 4. Results and discussion

### 4.1. Characterization

Fig. 4 shows the X-ray diffraction pattern of commercial $Mo_2C$ obtained using Co Kα radiation. As observed, the only

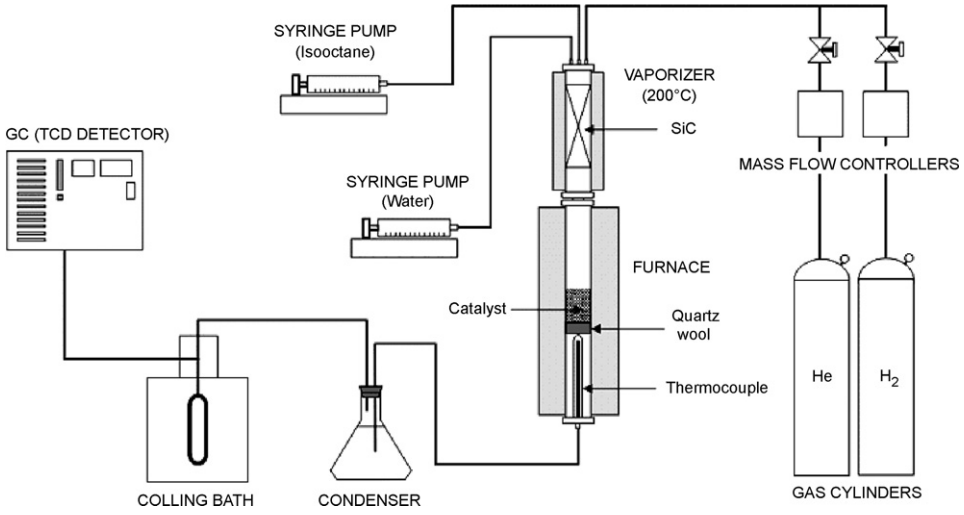


Fig. 3. Steam reforming reactor schematic.

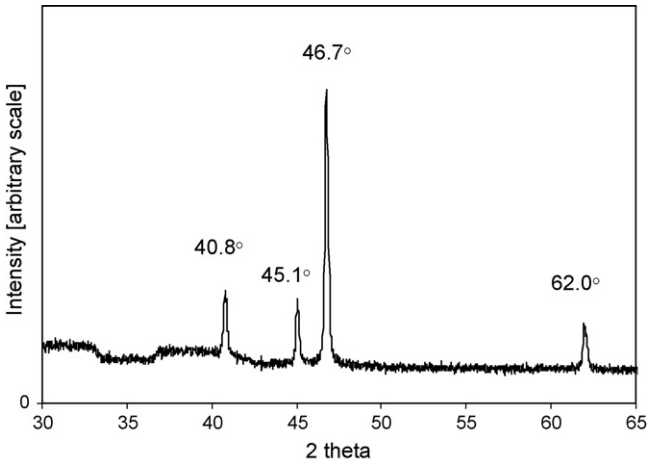


Fig. 4. XRD pattern of commercial $Mo_2C$.

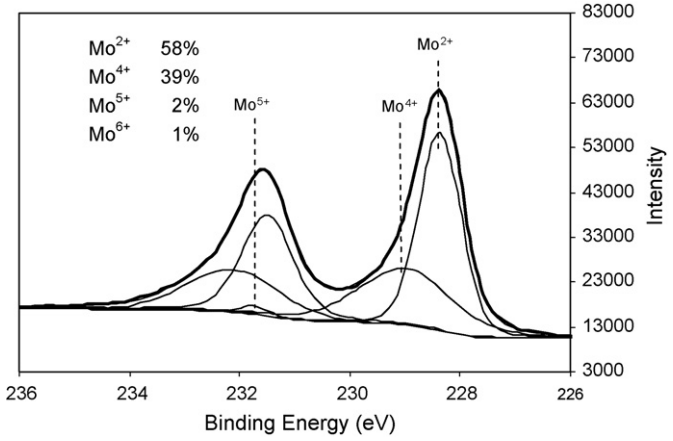


Fig. 6. Mo3d XPS spectrum of pretreated commercial $Mo_2C$.

phase detected in the bulk of the sample was β–$Mo_2C$. However, XPS analysis indicated that the catalyst surface not only consisted of the carbide phase ($Mo^{2+}$, 228.4 eV) but also the dioxide phase ($Mo^{4+}$, 229.5 eV), the oxycarbide phase ($Mo^{5+}$, 231.2 eV), and the trioxide phase ($Mo^{6+}$, 232.7 eV), as seen in Fig. 5. The surface area of the catalyst was determined using BET analysis and found to be 0.3 $m^2$/g.

### 4.2. $H_2$ pretreatment

The significant concentration of Mo atoms with oxidation degrees 5+ and 6+ on the catalyst surface can be substantially reduced by means of a pretreatment with $H_2$, which is intended to increase the concentration of the carbide phase and minimize those of the other phases. $H_2$ pretreatments are beneficial due to their ability to reduce excess carbon and eliminate the oxycarbide phase ($Mo^{5+}$) [17]. To investigate the effect of the $H_2$ pretreatment on the catalyst surface, 0.5 g of commercial $Mo_2C$ was subjected to a 20-min $H_2$ pretreatment, using a flow rate of 50 ml/min and a temperature of 850 °C. The pretreated sample was analyzed using XPS analysis and the XPS Mo3d spectrum obtained is displayed in Fig. 6. This analysis revealed that $H_2$ pretreatment was highly effective at reducing the concentration of the highest oxidation degrees existing on the catalyst surface, namely oxycarbide $Mo^{5+}$ and trioxide $Mo^{6+}$. On the other hand, the pretreatment was able to increase the concentration of carbide $Mo^{2+}$ from 15% to 58%, although the amount of the dioxide $Mo^{4+}$ also experienced a raise from 14% to 39%. In light of these results, we conclude that a short $H_2$ pretreatment is able to eliminate Mo with high oxidation degrees (5+, 6+), however, in doing so, the pretreatment appears to cause an increase in the concentration of the dioxide phase $Mo^{4+}$.

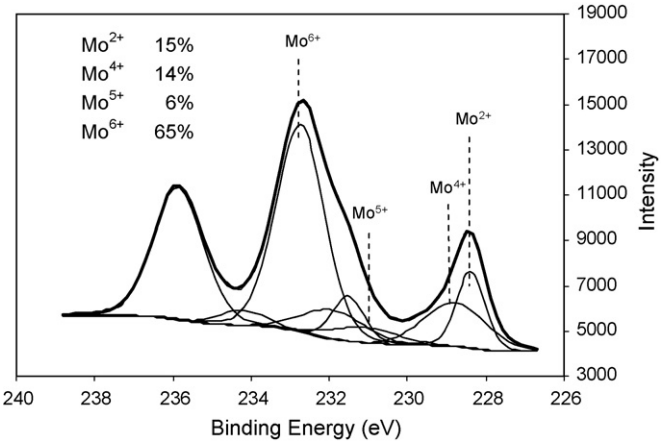


Fig. 5. Mo 3d XPS spectrum of commercial $Mo_2C$.

### 4.3. Catalytic activity

The catalytic activity of commercial $Mo_2C$ for isooctane steam reforming was measured at 850 °C, under different operating conditions. The variables investigated in the present work were the weight hourly space velocity (WHSV), defined as the ratio of mass flow rate to the mass of catalyst, and the steam to carbon molar ratio (S/C). The performance achieved under different values of these parameters and their effect on the catalytic activity, expressed in terms of hydrogen yield, is displayed in Fig. 7. As observed, high performances were obtained at spaces velocities smaller than 1.8 $h^{-1}$ and S/C ratios of about 1, which agrees with the thermodynamic analysis performed in Section 2. The ratio S/C = 1 corresponds to the

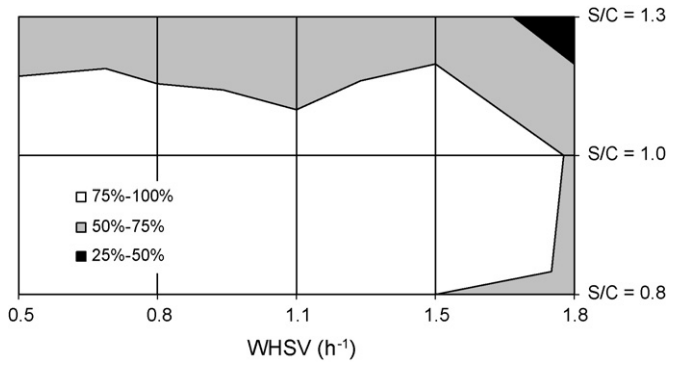


Fig. 7. Hydrogen yield as function of WHSV and S/C ratio (pretreated commercial $Mo_2C$, He = 10 sccm, $T$ = 850 °C).

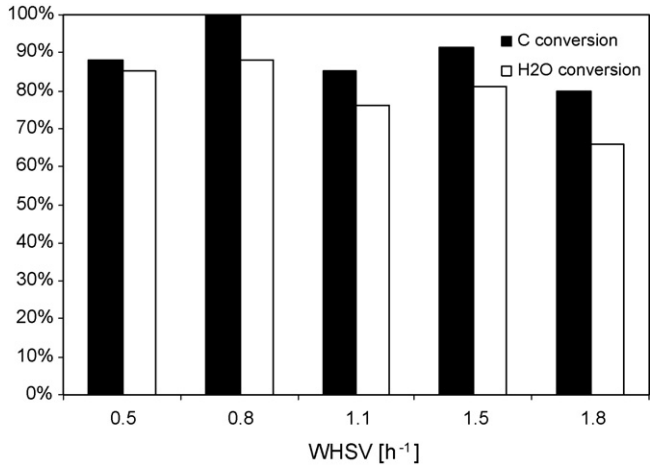


Fig. 8. Conversion as a function of WHSV at S/C = 1 (pretreated commercial $Mo_2C$, He = 10 sccm, S/C = 1, $T$ = 850 °C).

stoichiometric value indicated by reaction (1) and denotes that high concentrations of steam simply lead to unreacted water, rather than an improvement of the catalytic activity.

Fig. 8 shows the effect of the space velocity on the conversion at S/C = 1. The decline in the performance at higher space velocities can be related to the low surface area measured for the catalyst, which limits the contact area between the reactants and the catalyst surface. As observed, the conversions of isooctane and water appeared to be slightly reduced from 92% and 81% at WHSV = 1.5 $h^{-1}$, to 80% and 66%, at WHSV = 1.8 $h^{-1}$, respectively. This decrease may be attributed to the excess of reactants fed to the reactor, which were not completely converted to products.

The selectivity of $Mo_2C$ to the reforming products at S/C = 1 is reported in Fig. 9. As seen, the selectivity to $H_2$ and CO was held to values around 65% and 25% within the space–velocity range investigated in the present work. The average ratio $H_2$/CO was 2.57, which is higher than the value indicated by the stoichiometry of reaction (1), i.e., 2.13. This suggests that CO was consumed by one or more side reactions taking place in the reactor. The negligible evolution of $CO_2$ indicates that reactions like Boudart's or water–gas shift did not likely to happen to a significant extent, along with the reforming process. CO methanation would lead to $H_2$/CO ratios smaller than 2.13 and, therefore, this reaction did not likely occur either. The small concentration of other species produced during the reforming process (<10%) suggests that CO was probably consumed by unknown reactions to form compounds that were not considered in our analysis.

### 4.4. Effect of the temperature on the catalytic activity

The effect of operating temperature on the catalytic activity of commercial $Mo_2C$ was also investigated. Accordingly, an experiment consisting of two parts was carried out. In the first part, a fresh sample of commercial $Mo_2C$ was pretreated with hydrogen and then employed to perform isooctane steam reforming at 1000 °C, with WHSV = 0.5 $h^{-1}$, S/C = 1.3, and He as carrier gas. Once the catalytic activity was measured at 1000 °C, the temperature was decreased in 50 °C-steps and the performance was measured again at steady state conditions, which typically took 30 min. This procedure was repeated until the catalyst was no longer active, which happened at 650 °C. This inactive spent sample at 650 °C (denoted as sample 1) was cooled down to room temperature in flowing He, and then removed from the reactor for XPS analysis.

In the second part of the experiment, another fresh sample of commercial $Mo_2C$ was subjected to the same $H_2$ pretreatment and then used for isooctane steam reforming, which was started at 700 °C. The procedure was basically the same as in the first part, except that this time the temperature was systematically increased in 50 °C-steps up to 1000 °C. After the last measurement at 1000 °C, the sample was cooled down to room temperature in flowing He, and then removed from the reactor in order to acquire its XPS spectrum (denoted as sample 2). Fig. 10 shows the catalytic activity obtained in both parts of the experiment.

As observed, at temperatures of 850 °C and higher, the response of the catalytic activity in terms of hydrogen yield was practically the same, regardless of the direction from which the temperature was reached. For instance, the production of

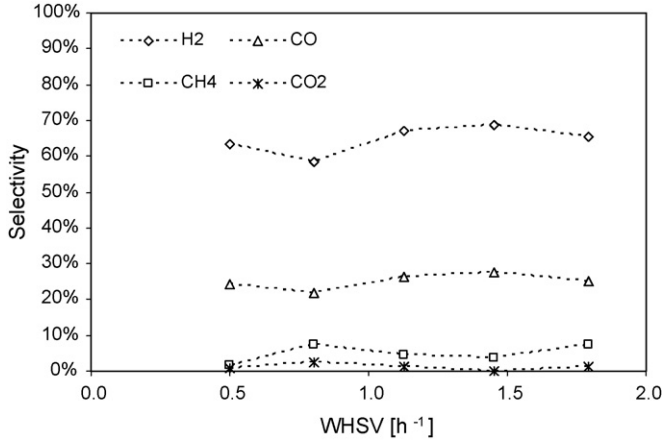


Fig. 9. Selectivity of $Mo_2C$ at S/C = 1 (pretreated commercial $Mo_2C$, He = 10 sccm, $T$ = 850 °C).

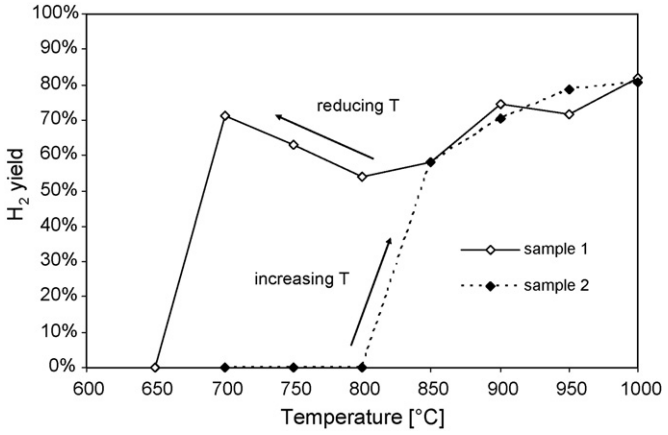


Fig. 10. Effect of the temperature on $Mo_2C$ catalytic activity.

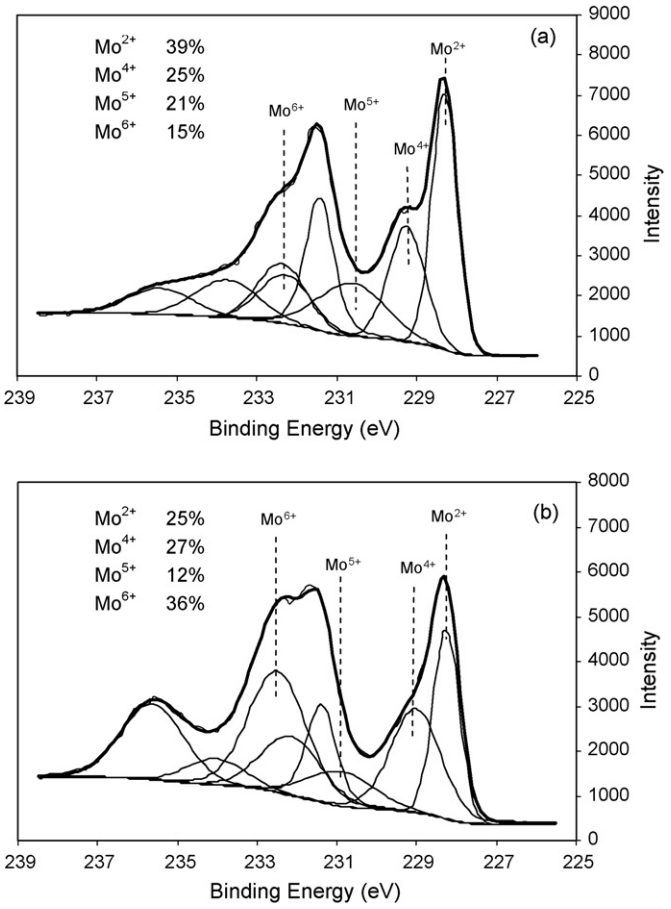


Fig. 11. XPS Mo3d spectra of (a) sample 1 (inactive spent catalyst at 650 °C) and (b) sample 2 (active spent catalyst at 1000 °C).

hydrogen measured at 850 °C was 58% from both directions. However, at reforming temperatures between 700 and 850 °C, their catalytic activities displayed significant differences. When the temperature was systematically decreased from 1000 to 650 °C, the catalyst showed high activity even at temperatures as low as 700 °C, where the hydrogen yield was 70%. Yet, when the temperature was increased from 700 to 1000 °C, the catalyst showed no activity until it reached 850 °C. The XPS spectra of sample 1 at 650 °C and sample 2 at 1000 °C are displayed in Fig. 11.

According to Fig. 11, the Mo3d spectrum of sample 1 (the inactive spent catalyst at 650 °C) exhibited a higher concentration of the carbide phase compared to that of sample 2 (the active spent catalyst at 1000 °C), which could indicate that the activity may not be directly related to the concentration of carbide on the catalyst surface. The dioxide peak displayed similar concentrations in the spectra of both samples. In addition, the oxycarbide peak was found in both samples. However, the intensity of this peak was higher in the spectrum of the inactive sample 1, which led us to consider a possible relationship between the appearance of the oxycarbide phase and the catalytic activity. In fact, when the catalyst exhibits poor activity, the concentration of unreacted isooctane in the environment is higher, and this increases the formation rate of the oxycarbide phase. The concentration of the trioxide phase was more elevated in the active sample 2 as compared to that found in the spectrum of the inactive sample 1. This decline in the trioxide concentration is due to its consumption in the formation the oxycarbide phase through combination with unreacted isooctane [13].

### 4.5. Analysis of the catalytic activity

This section is intended to provide an explanation for the phenomena reported earlier in this work. To start, a hypothesis intended to explain how the reforming process takes place will be suggested and, thereupon, all the experimental findings that support the hypothesis will be provided.

We hypothesize that isooctane steam reforming takes place via the following global reactions:

$$Mo_2C + 5H_2O \leftrightarrows 2MoO_2 + CO + 5H_2 \quad (2)$$

$$2MoO_2 + 0.51C_8H_{18} \leftrightarrows 2Mo_2C + 4.59H_2 + 2.16CO + 0.92CO_2 \quad (3)$$

Thus, the reforming process becomes stable as long as these reactions are continuously taking place. Reaction (2) has been considered by Darujati et al. [17] as the one causing the oxidation of $Mo_2C$ catalysts during steam reforming processes. Reaction (2) can be expressed as the result of the following 2-step mechanism:

- Step 1: Thermal decomposition of the carbide phase $Mo_2C$

$$Mo_2C \leftrightarrows 2Mo + C \quad \Delta H^\circ = +53.1\,kJ\,mol^{-1} \quad (4)$$

- Step 2: Oxidation of the products of step 1 with steam

$$Mo + 2H_2O_{(g)} \leftrightarrows MoO_2 + 2H_{2(g)} \quad \Delta H^\circ = -105.3\,kJ\,mol^{-1} \quad (5)$$

$$C + H_2O \leftrightarrows CO + H_2 \quad \Delta H^\circ = +131.3\,kJ\,mol^{-1} \quad (6)$$

Reaction (4) appears to be thermodynamically favored by high temperatures, as observed in Fig. 12. This is in agreement with a previous experimental study conducted by LaMont and Thomson, who found that the rates of decomposition of $Mo_2C$ become high at 750 °C and can cause the total disappearance of the carbide phase at 850 °C [16].

Darujati et al. found that the onset temperature of reaction (2) was 600 °C [17]. In the same studies, it was also noticed that reaction (2) appears to happen in two stages: at temperatures below 750 °C, the oxidation rates are independent of the $H_2O$ concentration and at temperatures of 750 °C and higher, the rate of reaction (2) increases as the concentration of steam becomes greater. As indicated by Fig. 12, reaction (2) is a process favored by high temperatures, which is in concordance with Darujati et al.'s experimental study.

Based on this information, the effect of the reforming temperature on the activity of $Mo_2C$ that is seen in Fig. 10 can be understood in terms of the thermal decomposition of the carbide phase. At low reforming temperatures, the thermal decomposition of the carbide phase, as described by reaction

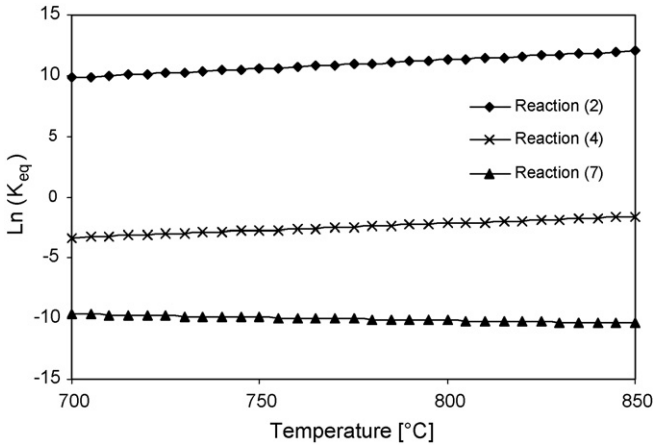


Fig. 12. Equilibrium constants.

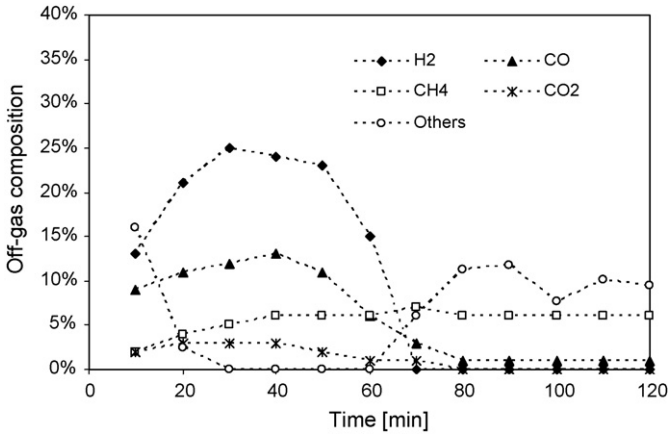


Fig. 13. Carburization of $MoO_2$ with isooctane at 700 °C.

(4), becomes kinetically limited as well as thermodynamically unfavorable and leads to low concentrations of $MoO_2$ on the catalyst surface. In turn, low concentrations of $MoO_2$ reduce the rates of reaction (3), therefore preventing the continuous oxidation and reduction of Mo metal according to reactions (2) and (3). Consequently, the initiation of the reforming process would never occur and the catalyst would become inactive for steam reforming of isooctane at low reforming temperatures. This explanation agrees with the findings reported in Fig. 10, where the pretreated commercial $Mo_2C$ showed no activity as the reforming temperature was raised from 700 to 800 °C. In addition, by further increasing the reforming temperature to 850 °C, the pretreated commercial $Mo_2C$ became active, which led us to think that, at that temperature, reactions (2) and (3) started to take over. The reforming rates at temperatures above 850 °C were limited by the available amount of Mo metal produced by the thermal decomposition. Thus, regardless of the direction at which the temperature was changed, the pretreated commercial $Mo_2C$ displayed the same catalytic activity at temperatures above 850 °C. According to Fig. 10, when the temperature decreased from 1000 to 650 °C, the pretreated commercial $Mo_2C$ was able to maintain its high catalytic performance even at reforming temperatures as low as 700 °C. This dependency of the catalytic performance on the temperature change direction within the range between 800 and 700 °C can be explained by considering the effect of the reforming environment. As the reforming temperature becomes lower than 850 °C, the $Mo_2C$ thermal decomposition rates become smaller. However, the hydrogen produced via the reforming process is able to enhance the decomposition of the carbide phase to form Mo metal through reaction (7), which activates the mechanism of reforming process described by reactions (2) and (3), even though the thermal decomposition of the carbide phase occurs at low rates:

$$Mo_2C + 2H_2 \leftrightarrows 2Mo + CH_4 \quad \Delta H^\circ = -21.6\,\mathrm{kJ\,mol^{-1}} \tag{7}$$

This reaction has been previously reported by other investigators [16] and found to take place between 650 and 800 °C. Based on this information, we believe that the high reforming performances obtained in Fig. 10, when reducing the temperature from 850 to 700 °C, are the direct result of reaction (7).

As indicated by Fig. 10, when the temperature was raised from 700 to 800 °C, no activity was detected using only He as the carrier gas. However, increasing the $H_2$ concentration in the feed stream of isooctane and water should improve the reforming performance by promoting the formation of Mo metal via reaction (7). To confirm this, isooctane steam reforming over commercial $Mo_2C$ was performed using $H_2$ along with He as the carrier gas at temperatures ranging from 700 to 800 °C. For each test, the WHSV and S/C ratio were set to 1 $h^{-1}$ and 1, respectively. At 800 °C, a flow of 10 sccm of $H_2$ was used as the carrier gas during the first 10 min of reforming, after which the carrier gas was switched to He at the same flow rate. The $H_2$ fed at the start of the experiment was sufficient to activate the catalyst and provoke a reforming performance which was stable for at least 1 h, with a hydrogen yield of 55%. At 750 °C, the same flow rate of $H_2$ was used as a carrier gas intended to enhance the reforming performance. However, unlike the experiment at 800 °C, the flow of $H_2$ had to be continuous in order to maintain a stable catalytic activity for at

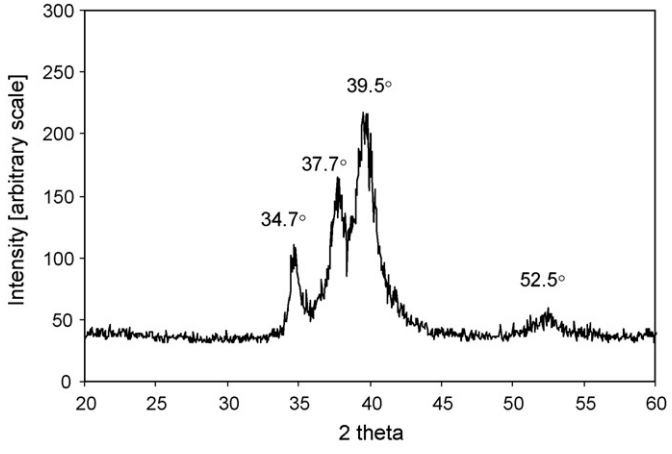


Fig. 14. XRD pattern of $MoO_2$ carburized with isooctane.

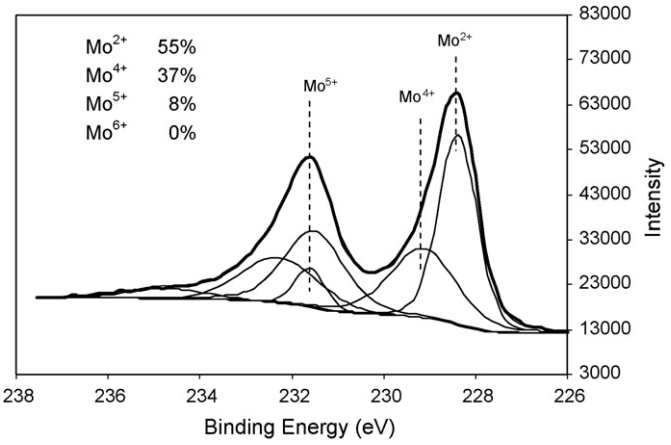


Fig. 15. XPS Mo3d pattern of $MoO_2$ carburized with isooctane.

least 1 h, with a hydrogen yield of 63%. At this temperature, switching the carrier gas to He only caused a significant drop in the reforming performance. Finally, at 700 °C, all the efforts to enhance the catalytic activity with $H_2$ were unsuccessful. Neither higher $H_2$ flow rates nor longer exposure times were able to activate the catalyst and increase the reforming rates. The results just described above may be interpreted by taking into consideration a kinetic approach. As the temperature decreases from 800 to 700 °C, reaction (7) becomes thermodynamically favored, as indicated by Fig. 12. However, reduction of the temperature results in a decline in the reaction rates, which appears to have a more significant impact on the reforming performance than that which is expected from thermodynamics.

The carburization of the oxide phase with isooctane, as described by reaction (3), has been investigated in the present work. To accomplish this, 0.5 g of commercial $MoO_2$ was placed into the reactor and combined with 1 ml/h of previously vaporized isooctane. The carburization was performed at 700 °C. Displayed in Fig. 13 is the evolution of the gas products as a function of time. The high reaction rates observed during the first 60 min of reaction indicate that this process was kinetically favored. Secondly, the declines in the concentrations of $H_2$ and CO indicate that the process had reached completion. From that point on, the solid formed through this reaction was catalytically converting isooctane into other compounds, which could not been identified by GC. To gain greater insight into the actual mechanism of the carburization process, further investigation is required. The stoichiometric coefficients appearing in reaction (3) are only approximations based on the concentrations of the products in the off-gas.

The solid phase obtained from the carburization process was analyzed using XRD with radiation Cu Kα, and XPS. The diffraction pattern shown in Fig. 14 denotes the presence of only $Mo_2C$ in the bulk phase [18], whereas the XPS Mo3d spectrum displayed in Fig. 15 indicates that the catalyst surface is composed of the carbide phase (55%), the dioxide phase (37%), and a minor amount of the oxycarbide phase (8%).

## 5. Conclusions

The onset temperature to perform isooctane steam reforming, using commercial $Mo_2C$ as the catalyst and He as the carrier gas, is 850 °C.

The catalytic performance obtained at 850 °C indicates that isooctane steam reforming is highly efficient at S/C ratios close to 1, in agreement with thermodynamic predictions. The space velocity (WHSV) appears to have an insignificant effect on the activity even at values as high as 1.8 $h^{-1}$.

The catalytic activity of $Mo_2C$ is initiated by the thermal decomposition of the carbide phase and propagated by the carburization of the dioxide phase with isooctane. The onset temperature of the reforming process is directly related to the temperature at which $Mo_2C$ is able to produce Mo metal. Under reducing environments with $H_2$ as the carrier gas, the production of Mo metal is enhanced, causing a reduction in the onset temperature to 750 °C.

## Acknowledgment

The authors are very thankful for the support of the WSU Foundation.

## References

[1] M. Wang, J. Power Sources 112 (2002) 307.
[2] D.J. Moon, J.W. Ryu, S.D. Lee, B.G. Lee, B.S. Ahn, Appl. Catal. A 272 (2004) 53.
[3] D.P. Papadias, Sh.H.D. Lee, D.J. Chmielewski, Ind. Eng. Chem. Res. 45 (2006) 5841.
[4] L.F. Brown, Int. J. Hydrogen Energy 26 (2001) 381.
[5] Q. Ming, T. Healey, L. Allen, P. Irving, Catal. Today 77 (2002) 51.
[6] A. Docter, A. Lamm, J. Power Sources 84 (1999) 194.
[7] S. Specchia, A. Cutillo, G. Saracco, V. Specchia, Ind. Eng. Chem. Res. 45 (2006) 5298.
[8] A. Esroz, H. Olgun, S. Ozdogan, J Power Sources 154 (2006) 67.
[9] J. Zhang, Y. Wang, R. Ma, D. Wu, Appl. Catal. A 243 (2003) 251.
[10] A.A. Praharso, D.L. Adesma, N.W. Trimm, Cant. Chem. Eng. J. 99 (2004) 131.
[11] L. Wang, K. Murata, Y. Matsumura, M. Inaba, Energy Fuels 20 (2006) 1377.
[12] A.P.E. York, A.J. Brungs, S.C. Tsang, M.L.H. Green, Chem. Commun. 40 (1997) 39.
[13] C. Pham-Huu, M.J. Ledoux, J. Guille, J. Catal. 143 (1993) 249.
[14] P. Cheekatamarla, W.J. Thomson, J. Power Sources 156 (2006) 520.
[15] P. Cheekatamarla, W.J. Thomson, Appl. Catal. A 287 (2005) 176.
[16] D.C. LaMont, W.J. Thomson, Appl. Catal. A 274 (2004) 173.
[17] A.R.S. Darujati, D.C. Lamont, W.J. Thomson, Appl. Catal. A 253 (2003) 397.
[18] T. Xiao, A.P.E. York, K.S. Coleman, B. John, J. Claridge, J. Sloan, M.L.H. Charnok, Green, J. Mater. Chem. 11 (2001) 3094.